F. Ebrahimi, N.A. Windarko, A.I. Gunawan

Wild horse optimization algorithm implementation in 7-level packed U-cell multilevel inverter to mitigate total harmonic distortion

*Introduction. Multilevel inverters (MLIs) are a popular industrial and, more especially, renewable energy application solution. This is because of its appetite for filters, low distortion class, and capacity to provide a multilayer output voltage that resembles a pure sine waveform. **The novelty** is in applying the wild horse optimization algorithm (WHOA) to adjust the sinusoidal pulse width modulation (SPWM) technique by producing the optimal reference signal parameters in a new multilevel inverter architecture known as the packed U-cell multilevel inverter (PUC-MLI). **Purpose.** This study helps with the idea of new inverter architecture and a modified pulse width modulation (MPWM) method to make the multilevel inverter smaller, cheaper, and with less total harmonic distortion (THD). **Methods.** We use the proposed approach to control a 7-level, single-phase PUC-MLI. The WHOA is used to discover the optimal parameters of the additional reference sine signal after being compared with SPWM to evaluate its performance in harmonic reduction. The simulation's outcome was validated by building a PUC-MLI prototype. **Results.** Experimental results and simulations validate the effectiveness of the suggested approach. The WHOA-improved MPWM approach achieves a significant reduction in THD on the PUC-MLI output voltage, as indicated by the results. **Practical value.** THD in MLI output voltage will be reduced without spending any cost. The suggested solution works with many MLI topologies with varying output voltage levels. References 20, tables 6, figures 12.*
Key words: **packed U-cell multilevel inverter, total harmonic distortion, modified pulse width modulation, wild horse optimization algorithm.**

*Вступ. Багаторівневі інвертори (MLIs) є популярним рішенням для застосування у промисловості та, особливо, у відновлюваних джерелах енергії. Це пов'язано з його потребою у фільтрах, низьким класом спотворень та здатністю забезпечувати багатошарову вихідну напругу, що нагадує чистий синусоїдальний сигнал. **Новизна** полягає у застосуванні алгоритму оптимізації «дикого коня» (WHOA) для налаштування методу синусоїдальної широтно-імпульсної модуляції (SPWM) шляхом створення оптимальних параметрів опорного сигналу в новій архітектурі, відомої як упакований багаторівневий інвертор U-подібного типу (PUC-MLI). **Мета.** Це дослідження допомагає реалізувати ідею нової архітектури інвертора та модифікованого методу широтно-імпульсної модуляції (MPWM), що дозволяє зробити багаторівневий інвертор меншим, дешевшим і з меншим загальним гармонічним спотворенням (THD). **Методи.** Ми використовуємо запропонований підхід для керування 7-рівневим однофазним PUC-MLI. WHOA використовується для визначення оптимальних параметрів додаткового еталонного синусоїдального сигналу після порівняння зі SPWM для оцінки його ефективності зниження гармонік. Результати моделювання були підтверджені створенням прототипу PUC-MLI. **Результати.** Експериментальні результати та моделювання підтверджують ефективність запропонованого підходу. Удосконалений WHOA підхід MPWM дозволяє досягти значного зниження THD вихідної напруги PUC-MLI, про що свідчать результати. **Практична цінність.** THD вихідної напруги MLI буде знижено без будь-яких витрат. Пропоноване рішення працює з багатьма топологіями MLI з різними рівнями вихідної напруги. Бібл. 20, табл. 6, рис. 12.*
Ключові слова: **упакований багаторівневий інвертор U-cell, повне гармонічне спотворення, модифікована широтно-імпульсна модуляція, алгоритм оптимізації «дикого коня».**

Abbreviations

CHB	Cascaded H-bridge	PUC	Packed U-cell
FFT	Fast Fourier Transform	PUC-MLI	Packed U-cell Multilevel Inverter
FLC	Flying Capacitor	PWM	Pulse Width Modulation
MPWM	Modified Pulse Width Modulation	SPWM	Sinusoidal Pulse Width Modulation
MLI	Multilevel Inverter	THD	Total Harmonic Distortion
NPC	Neutral Point Clamped	WHOA	Wild Horse Optimization Algorithm

Introduction. Afghanistan, one of the least developed nations, has serious economic problems. Industry is essential to its growth, but the lack of power impedes development because of an imbalance between supply and demand. Afghanistan has a lot of solar potential, so the government is pursuing a 2000 MW renewable energy initiative as a solution to this. By allowing the establishment of factories in isolated locations without long transmission lines, solar energy may stimulate the local economy. The factory needs electricity in the AC range. Inverters are devices that change DC voltage into AC voltage. The application of inverters is wide; however, it can be used where DC power is a supplier and AC power is the consumer; for instance, it can be used for renewable energy applications. Grid-connected or standalone systems widely use MLIs as voltage converters to provide AC loads with power from renewable energy sources such as wind turbines and solar panels [1]. High-efficiency power conversion systems achieve exceptional performance by minimizing THD and reducing conduction losses during switching; these systems can maximize their energy conversion capacities and achieve improved overall efficiency and performance by regulating these elements properly [2].

Because the MLI can generate output waveforms with lower THD and higher quality, they are becoming more and more popular. Electrical loads in the AC output voltage require a sinusoidal waveform. All the same, MLI may provide an output voltage that looks like a staircase and is almost exactly like a sine wave. The generation of switching patterns results in an output voltage from the staircase that is not a perfect sine wave. The staircase sine wave contains harmonics. Researchers have developed other MLI variants, including PUC-MLI, FLC MLI and CHB MLI to address this problem [3]. The complex structure of MLI circuits has led some academics to recommend reducing the number of components in them [4]. Even still, the PUC-MLI architecture necessitates a low quantity of devices in order to provide a high output voltage among MLIs [5] that will address the size and cost of construction of MLI issues.

The efficient control of switching patterns to reduce the THD of the output voltage is a major area of active study in MLIs, in addition to the exploration of topological solutions [6]. Space vector modulation [7], selective harmonic elimination, PWM [8] are some of the methods that have been suggested to reduce THD in MLI. Lower-order harmonic suppression in the straight-line output voltage of MLIs has been the explicit focus of several reported modulation techniques [9]. It is also standard practice to use injection techniques that include the modulated signal's integration of several reference signals [10].

In order to reduce THD in MLI, several studies have suggested novel injection techniques. The third harmonic injection space vector PWM [11], the third harmonic injection PWM [12], and the generalized discontinuous PWM [13] are a few instances of distinct PWM approaches. Each strategy significantly impacts the THD value of the output voltage.

Recently, researchers have optimized the THD of the output voltage in MLI by applying meta-heuristic methods in modulation approaches. Particle swarm optimization was used in [14] to improve the design of grid-connected photovoltaic systems. The whale optimization algorithm has been used in PUC-MLI to reduce the THD of the output voltage of MLI; the result is presented only in MATLAB simulation [15], and the researcher modified the switching pattern of MLI in order to reduce the THD in [16] focused on using evolutionary algorithms to get rid of harmonics in PUC-MLI. The result was presented through the simulation only as well; in another study, the researcher analyzed the THD of CHB MLI [17], and in another study, the grey wolf optimizer was used to improve the switching sequence of the NPC MLI in order to reduce the THD. They succeeded in reducing THD from 31.42 % to 26.44 % [18]. However, they used a grey wolf optimizer to optimize only 2 parameters of the injected signal, which are amplitude and phase shafted angle. Unfortunately, no studies have been done on the use of WHOA in PUC-MLI injection technique optimization, where the simulation result is confirmed by building a prototype PUC-MLI.

The goal of the paper. Utilizing the WHOA to optimize injection procedures in PUC-MLI has yet to be the subject of any study. This research aims to improve all parameters of the injected sine signal and lower THD in PUC-MLI by presenting a novel method that uses the WHOA. We will build and test a prototype PUC-MLI to verify the efficacy of the suggested approach. This will validate the simulation results and show how the WHOA will be used in practice to optimise switching patterns in PUC-MLI's switches.

Subject of investigations. The application of WHOA to optimize the injected signal parameters (amplitude, frequency and phase shifted angle) for a 7-level PUC-MLI is the focus of the study. Building a prototype, PUC-MLI will be used to validate the modelling outcome.

Methodology. Packed U-cell multilevel inverter. An electronic device or circuit that changes DC voltage into AC voltage is known as an inverter. Conventional inverters often offer 3 output voltage levels: zero, negative and positive states of output voltages ($-V_{dc}$ and $+V_{dc}$). An MLI is a type of special inverter that can simultaneously produce different voltage and current levels. Table 1 shows the number of devices required by different types of inverters (NPC, FLC, CHB) and PUC-MLI to achieve 7 output voltage levels.

Table 1

The number of devices corresponding to various categories of MLIs

Components	FLC	NPC	CHB	PUC
IGBTs	24	24	12	6
Capacitors	30	6	3	2
Clamping diodes	0	20	0	0
Total component	54	50	15	8

The PUC-MLI architecture requires only 8 devices to generate 7 output levels. By comparison, the NPC needs 50 devices, the FLC needs 54 and the CHB needs 15. Because of the U-shaped architecture of each unit, the inverter is called a «packed U-cell». Depending on the number of voltage sources (capacitors) and switches utilized, the voltage levels in the packed U-cell design may change. First presented the recommended inverter in 2010, which was then improved upon in 2022 [19]. The PUC-MLI design, which produces 7 output voltage levels by using 2 DC voltage sources and 6 switches, is shown in Fig. 1.
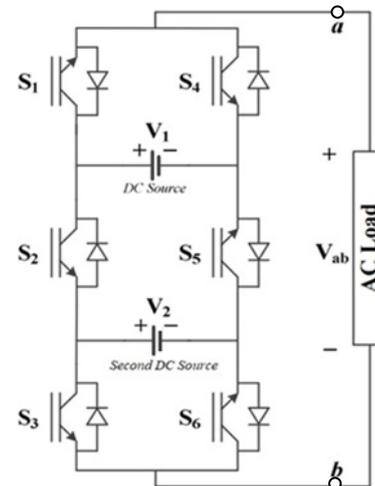

Fig. 1. PUC-MLI design

Table 2 states that this study suggests building a single-phase PUC-MLI structure with 8 output voltage states, which is constructed based on a sequence of connections between cells. As a precaution against DC bus short circuits, switches S4, S5 and S6 in Table 2 function in reverse relative to S1, S2 and S3. Even though the PUC may produce different voltage levels from different DC sources, in order to achieve maximum output voltage (V_{ab}), the second DC bus amplitude must be one-third of the first ($V_1 = 3V_2$). V_{ab} has 7 voltage levels as a result of this configuration: $0, \pm V_2, \pm 2V_2, \pm 3V_2$.

Table 2

PUC-MLI produces voltage levels

S1	S2	S3	S4	S5	S6	V_{ab}
1	0	0	0	1	1	V_1
1	0	1	0	1	0	$V_1 - V_2$
1	1	0	0	0	1	V_2
1	1	1	0	0	0	0
0	0	0	1	1	1	0
0	0	1	1	1	0	$-V_2$
0	1	0	1	0	1	$V_2 - V_1$
0	1	1	1	0	0	$-V_1$

Modified PWM technique. The presence of harmonic distortion in the output voltage of the PUC-MLI is a direct consequence of the switching process. As such, the use of a suitable modulation approach becomes imperative in order to reduce the negative impacts of harmonic distortion. A viable remedy is presented in this research paper – the MPWM approach. While the standard method of modulation is SPWM, it compares the triangle carrier signal with the sine reference signal. In the case of PUC-MLI only a few semiconductor components are required, specifically one reference signal and 6 carrier signals. Figure 2 demonstrates the MPWM techniques.
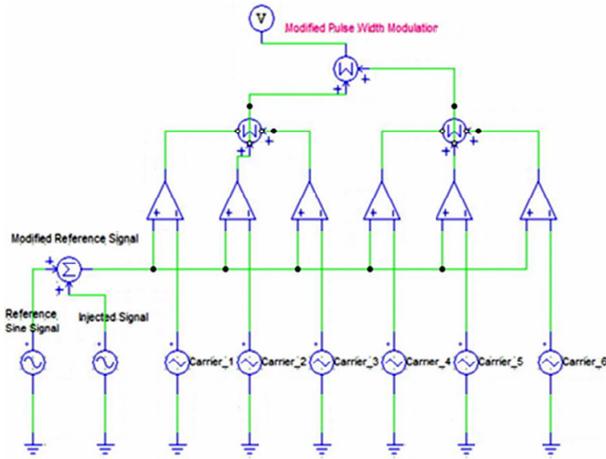
Fig. 2. The procedure for MPWM

The reference sine signal is altered when the injected sine signal and the reference sine signal are added together. The injected sine signal contains parameters for frequency, phase shift and amplitude, whereas the reference signal is a sinusoidal waveform with a fundamental frequency. The injected signal might be either a singular signal or numerous signals. The mathematical expressions representing these signals are as follows:

$$S_r(t) = A_1 \sin(2\pi f_1 t); \tag{1}$$

$$S_i(t) = \sum_{n=2}^{\infty} A_n \sin(2\pi f_n t + \theta_n), \tag{2}$$

where $S_r(t)$ is the reference signal; $S_i(t)$ is the injected signal.

Equation (1) represents a sinusoidal reference signal with amplitude A_1 of 3 and a fundamental frequency f_1 of 50 Hz. The signal in (2) represents the injected signal. The objective of the injected signal is to alter the reference waveform. The signal is characterized by its amplitude A_n, frequency f_n and phase shift θ_n. These parameters will be determined through the process of wild horse optimizer tracking to find their optimal values. Two signals are combined, yielding the mathematical expression in (3), as exemplified in (4):

$$S_M(t) = A_1 \sin(2\pi f_1 t) + \sum_{n=2}^{\infty} A_n \sin(2\pi f_n t + \theta_n); \tag{3}$$

$$S_M(t) = 3\sin(2\pi 50 t) + \sum_{n=2}^{\infty} 0.35 \sin(2\pi 999.72 t + 4.80); \tag{4}$$

where $S_M(t)$ is the modified signal.

The process of generating MPWM is depicted in Fig. 3. Figure 3,*a* depicts a sine wave that serves as a reference as stated in (1). The wave has amplitude of 3, a frequency of 50 Hz and a phase-shifted angle of 0. Figure 3,*b* shows a signal waveform that has been injected according to (2). This waveform has amplitude of 0.35 V, a frequency of 999.72 Hz and a phase shift of 271.37° (equivalent to 4.80 rad). Both signals are shown in Fig. 3,*c*. They are combined to make a new reference signal, which is shown in (3). This signal will be compared to the triangular carrier signal in the form of MPWM.
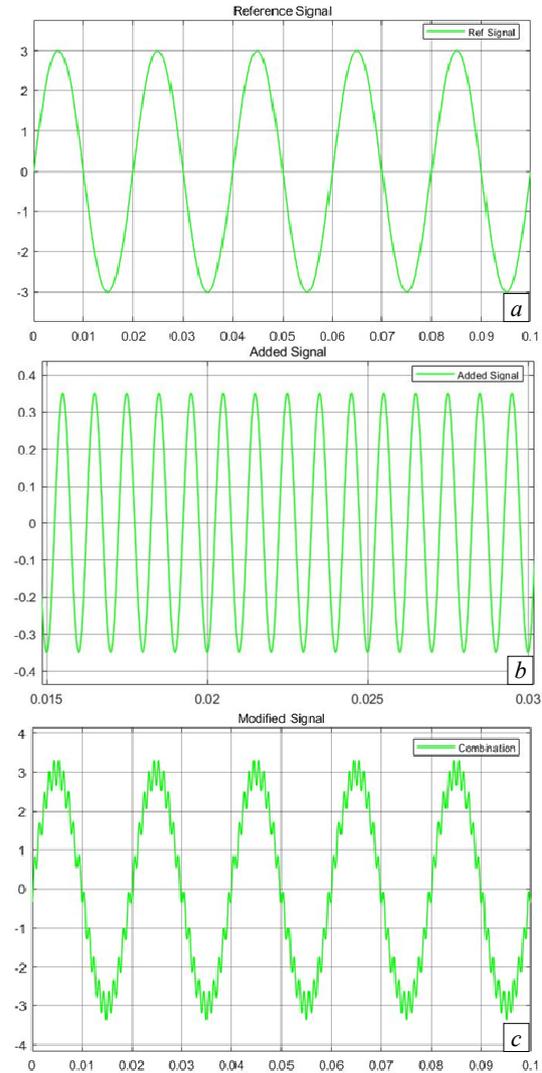

Fig. 3. MPWM signal generation process demonstrates:
a – the reference sine signal; *b* – the injected signal;
c – the modified reference signal

Wild horse optimization algorithm. The WHOA is a meta-heuristic optimization method that draws inspiration from wild horse behaviour. A dominant stallion leads a group of horses, and other horses (foals and mares) follow him. This social hierarchy and herd behaviour of wild horses are the basis for the algorithm [20]. A stallion is in charge of the herd of wild horses, which also includes mares and foals. The suggested method in this study is implemented as a flowchart (Fig. 4). According to this algorithm, like all meta-heuristic algorithms, starts with population initialization. This creates the first group of possible solutions, each represented by a set of values for the injected signal's amplitude, frequency and phase angle. Then, the fitness of each candidate solution is evaluated by

injecting its corresponding signal into the reference sinusoidal signal and measuring the performance of the modified switching pattern.
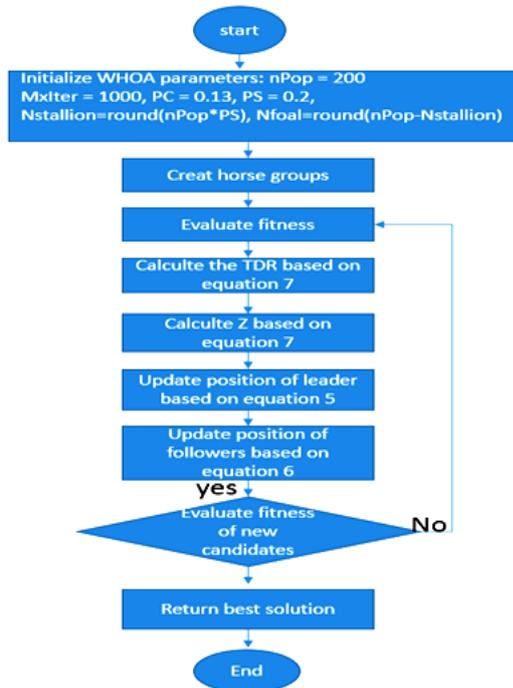

Fig. 4. Flowchart of the WHOA

After that, update the position of the leader, select the best candidate solution as the leader, and update its position using (5). Evaluate the fitness of the new candidate solutions generated using the following equations. Then repeat searching for a set number of iterations, updating the positions of the leader and followers using (6) at each iteration. Finally, return the best of the found solutions. After finding the modified value, evaluate the performance of the optimized switching pattern, add the modified signal to the reference sinusoidal signal, and measure the performance of the modified switching pattern using the MATLAB simulation FFT analyzer tool. The equations are:

$$\overrightarrow{Stallion_{Gi}} =$$
$$= \begin{cases} 2Z\cos(2\pi RZ)\cdot\left(WH - Stallion_{Gi}\right) + WH; \text{ if } R3 > 0.5; \\ 2Z\cos(2\pi RZ)\cdot\left(WH - Stallion_{Gi}\right) - WH; \text{ if } R3 \le 0.5, \end{cases} \quad (5)$$

where the subsequent location of the i group's leader, indicated as $\overrightarrow{Stallion_{Gi}}$, is established based on the present coordinates of the leader $Stallion_{Gi}$, the location of the water hole (WH), a dynamically computed adaptive mechanism (Z) utilizing (7), a uniformly distributed random number (R) ranging from –2 to 2.

Updating the positions of the followers can be done by comparing the positions of the remaining candidates based on their distance from the leader and a random term. The position of a follower is updated using (6):

$$\overrightarrow{X_{i,G}^{j}} = 2Z\cos(2\pi RZ)\cdot\left(Stallion^{j} - X_{i,G}^{j}\right) + Stallion; \quad (6)$$

$$P = \overrightarrow{R1} < TDR; \ IDX = P = 0; \ Z = R2\theta IDX + \overrightarrow{R3}\theta(\sim IDX), \quad (7)$$

where the variable $X_{i,G}^{j}$ signifies the current position of a group member, whether it's a foal or a mare. The notation $Stallion^{j}$ is employed to denote the location of the stallion, who serves as the group's leader. Z is a variable that dynamically changes depending on the size of the problem; it is not a continuous value. It is an essential component of the wild horse optimizer's scalability because of its function as a mechanism, which allows the algorithm to retain constant performance across various issue dimensions. It can be define as adaptive mechanism calculated through the use of (7). R is a randomly generated number with a uniform distribution within the range of [–2, 2], determining the angles at which horses graze around the group leader in a 360° fashion. Lastly, $\overrightarrow{X_{i,G}^{j}}$ indicates the updated position of a group member during grazing, as elaborated in reference [20].

Simulation results. MATLAB program is utilized for simulating the improved MPWM approach using an algorithm. The simulation utilizes the PUC-MLI with settings specified in Table 3.

Table 3
Simulation parameters for PUC-MLI

Components	Value
V_{DC1}	180
V_{DC2}	60

The initial DC supply values are 180 V for the first supply and 60 V for the second supply. To streamline the optimization process, the injected signal was treated as a singular waveform. WHOA optimizes the injected signal's frequency, amplitude and phase shift. Figure 5 displays an illustration of the outcomes of the tracking procedure for the injected signal. Figure 5,a represents the WHOA tracking process to find the best amplitude; Fig. 5,b represents the tracking process for the frequency; Fig. 5,c represents the tracking process for the phase shift of the added signal; and Fig. 5,d illustrates the THD reduction over iterations. All parameters, such as amplitude, frequency and phase shift are searched starting from 0 and then approached to their best value.
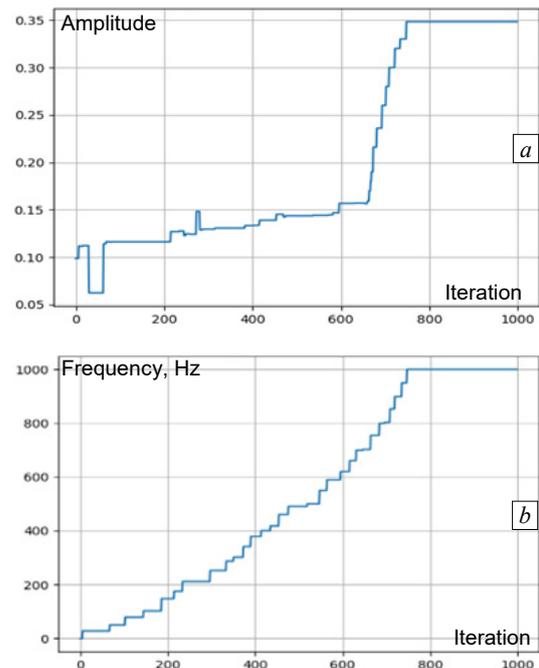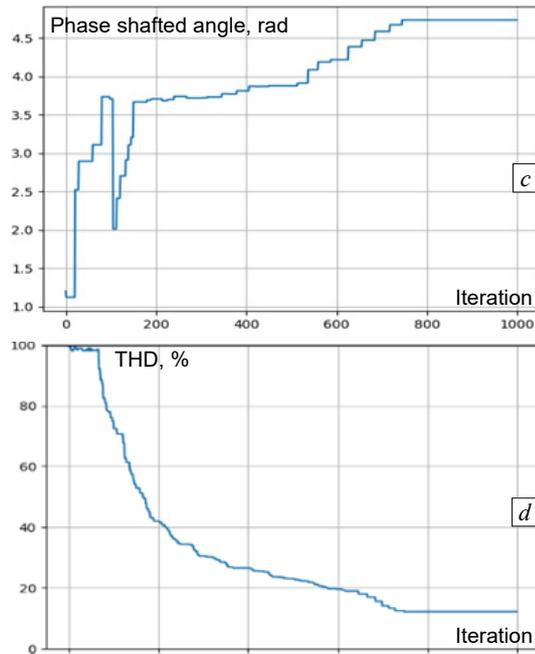
Fig. 5. Simulation results of the optimized injected signal

WHOA's performance was assessed against SPWM, resulting in a decrease in THD from 17.89 % to 12.25 %. To prevent getting trapped in local optima, WHOA was executed a hundred times, and the outcomes are presented in Fig. 6, where THD exceeds SPWM are marked as errors and highlighted with a chocolate colour bar chart. Conversely, lower THD values than SPWM signify success, but not the optimal solution, marked with a yellow colour bar chart, and the best solutions (global optima) are highlighted with a black colour bar chart. WHOA successfully attained the global optimum by reducing THD to 12.25 %. The values for amplitude, frequency, and phase-shift angle derived from WHOA were $A = 0.35$, $f = 999.72$, $\theta = 4.80$, detailed in Fig. 5,a–c.
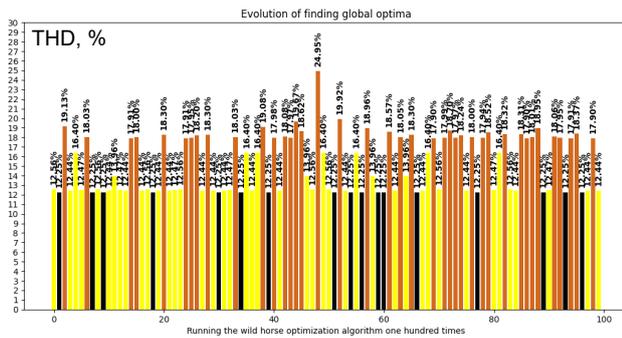

Fig. 6. The procedure for identifying global optima

The corresponding result is shown in Fig. 8,b. A comparison between the PUC-MLI output voltage waveform using SPWM and MPWM was conducted in MATLAB/Simulink. As both output voltages possess the same amplitude modulation, distinctions in the effects of the injected signal on MPWM can be identified by analyzing different patterns. Figure 7 demonstrates the inverter's output voltage – Fig. 7,a represents the inverter output in SPWM, while Fig. 7,b illustrates the output using MPWM.

Table 4 furnishes a comparison of THD levels in the PUC-MLI's output voltage, showing SPWM at 17.89 % and MPWM at 12.25 %.
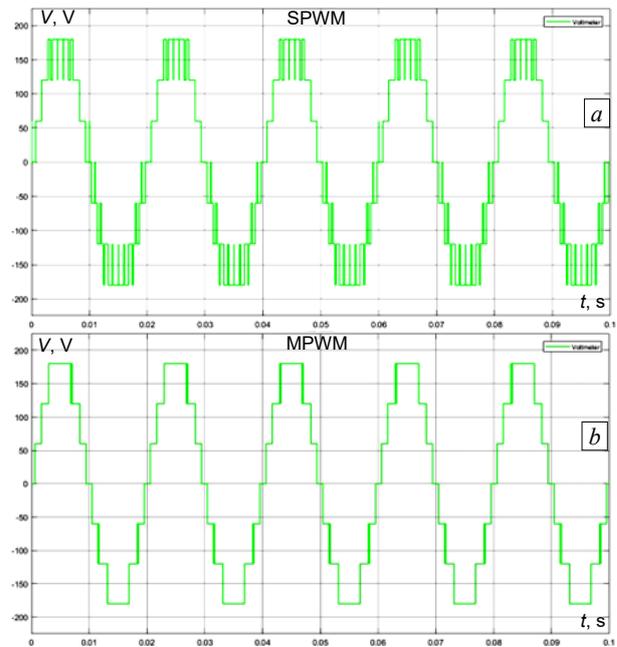

Fig. 7. Voltage output of PUC-ML

Table 4
Comparison of THD for the modulation technique

Modulation technique	THD, %
SPWM	17.89
MPWM	12.25

Furthermore, Fig. 8,a illustrates the harmonic spectrum of SPWM, while Fig. 8,b depicts the harmonic spectrum of the MPWM.
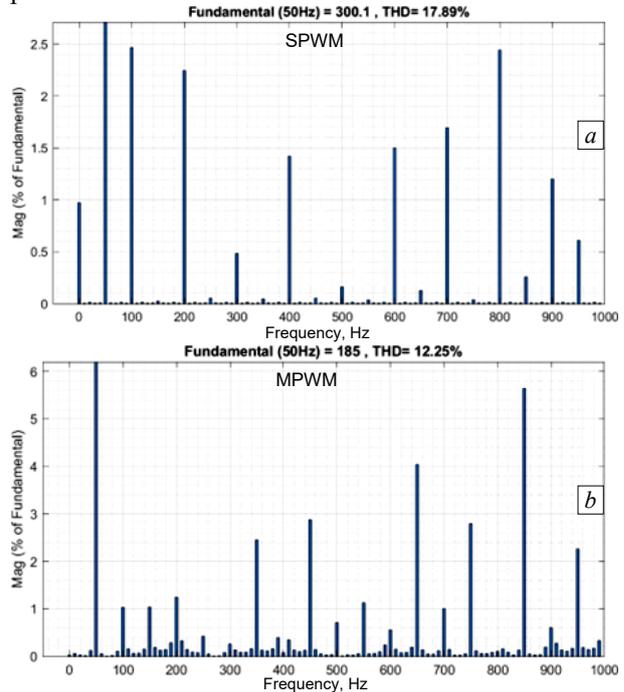

Fig. 8. Spectral analysis of harmonics

Experimental results. To confirm the WHOA's simulation findings and the recommended modulation strategy, a single-phase, 7-level PUC-MLI prototype was built. Software called AutoCAD Eagle was used to design the inverter. Table 5 lists the components that went into building PUC-MLI. Figure 9 shows the experimental system configuration and a close-up of PUC-MLI, shown in Fig. 10, respectively. For PUC-MLI switches, the

STM32F407G microcontroller on the Discovery board has generated switching pulses. This microcontroller is programmed using the C programming language and STM32CubeIDE version 1.1 software. The waveform and harmonic spectrum are measured and analyzed using a Rigol DS 1052E oscilloscope; the data from the oscilloscope is recorded, and then the amount of THD is measured using MATLAB software. Two programmable DC power sources that maintain a steady DC voltage (TDK-Lambda and GW Instek PSS-3203) supply the PUC-MLI. PUC MLI is tested with 2 DC input voltages, 20 V and 60 V, and a 500 W resistive load (see Fig. 9).

Table 5
Inventory of components utilized in the experiment

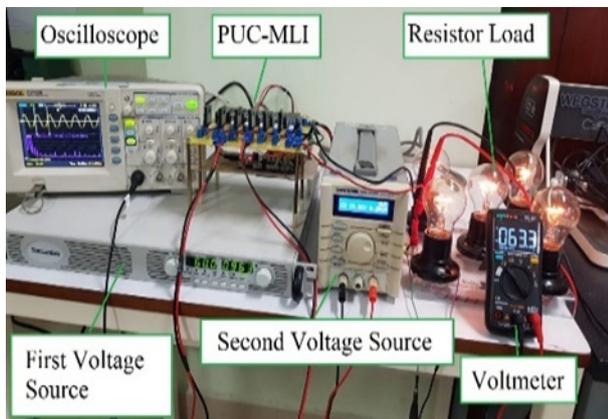| Components	Specifications
IGBT Switches	SGL160N60UFD (Faichild)
Microcontroller	Discovery STM32F407G
Optocoupler	FOD3182
Gate Drive Power Supply	DC 12V, HLK-PM12

Fig. 9. Arrangement and configuration of the experimental setup

Fig. 10. PUC-MLI hardware

The prototype PUC-MLI is utilized to validate the modulation of both SPWM and MPWM techniques using the optimal parameters obtained from simulation results. Both SPWM and MPWM are applied with an amplitude modulation of 1. In addition, the MPWM incorporates a 999.72 Hz injected signal with amplitude of 0.35 V and a phase shift of 271.37°. Figures 11,*a,b* present the experimental comparison between the output voltage of SPWM and MPWM, which aligns with the simulation results (see Fig. 7). The THD is determined by recording the output voltage. Figure 12 illustrates the spectrum and THD results, indicating that both modulation techniques exhibit a low-level harmonic spectrum at high frequencies. This high-frequency harmonic content offers an advantage in distortion suppression by employing a compact LC filter.

Notably, the THD of the MPWM, as listed in Table 6, measures 16.84 %, demonstrating that the optimized WHOA-based switching of the MPWM achieves a lower THD compared to SPWM, which has a THD of 18.44 %, which is a great success.
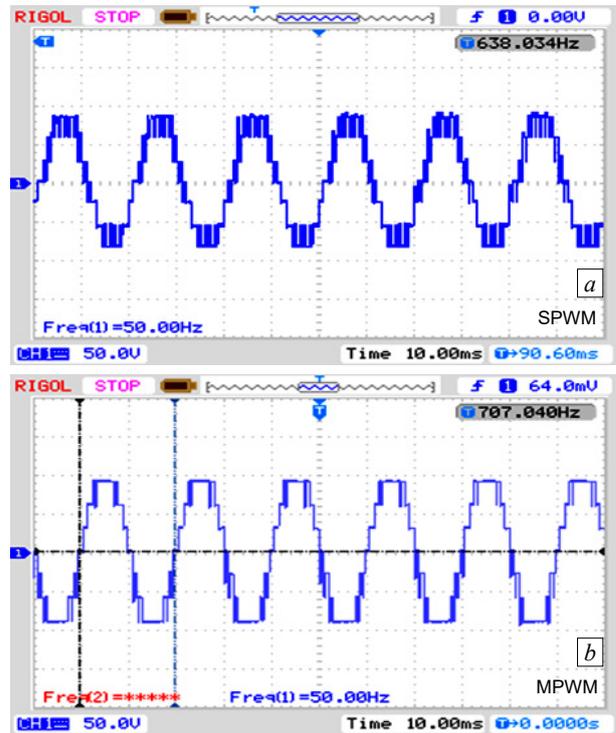

Fig. 11. The output voltage of PUC-MLI observed on the oscilloscope: *a* – SPWM; *b* – MPWM
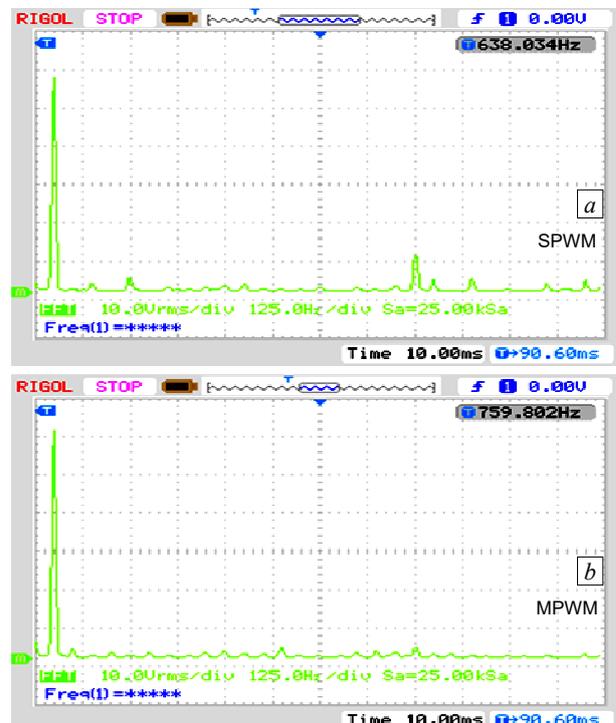

Fig. 12. Measurement of THD using the oscilloscope's FFT tools: *a* – THD of SPWM; *b* – THD of MPWM

Table 6
Experimental results for THD measurements

Method	THD, %
SPWM	18.44
MPWM	16.84

Conclusions.

1. Based on the findings of this research, the PUC topology of MLI is the best topology against other topologies of MLI, namely CHB, FLC and NPC, in order to overcome the size and cost of construction issues.

2. The WHOA can effectively reduce the THD in a PUC-MLI by improving the switching pattern of the inverter's switches. To validate this conclusion, a prototype PUC-MLI was built, and the proposed method was implemented.

3. The performance of the WHOA algorithm was compared with the SPWM in terms of THD reduction. The results indicate that the WHOA algorithm outperformed SPWM in terms of THD reduction performance. Therefore, the WHOA algorithm is a promising approach for reducing THD in PUC-MLIs.

4. Moreover, the reduced THD of PUC-MLI can support the advancement of applications for electrical vehicles in industry as well as renewable energy.

Conflict of interest. The authors declare that they have no conflict of interest.

REFERENCES

1. Bughneda A., Salem M., Richelli A., Ishak D., Alatai S. Review of Multilevel Inverters for PV Energy System Applications. *Energies*, 2021, vol. 14, no. 6, art. no. 1585. doi: https://doi.org/10.3390/en14061585.
2. Leon J.I., Vazquez S., Franquelo L.G. Multilevel Converters: Control and Modulation Techniques for Their Operation and Industrial Applications. *Proceedings of the IEEE*, 2017, vol. 105, no. 11, pp. 2066-2081. doi: https://doi.org/10.1109/JPROC.2017.2726583.
3. Harbi I., Rodriguez J., Liegmann E., Makhamreh H., Heldwein M.L., Novak M., Rossi M., Abdelrahem M., Trabelsi M., Ahmed M., Karamanakos P., Xu S., Dragičević T., Kennel R. Model-Predictive Control of Multilevel Inverters: Challenges, Recent Advances, and Trends. *IEEE Transactions on Power Electronics*, 2023, vol. 38, no. 9, pp. 10845-10868. doi: https://doi.org/10.1109/TPEL.2023.3288499.
4. Omer P., Kumar J., Surjan B.S. A Review on Reduced Switch Count Multilevel Inverter Topologies. *IEEE Access*, 2020, vol. 8, pp. 22281-22302. doi: https://doi.org/10.1109/ACCESS.2020.2969551.
5. Vahedi H., Al-Haddad K. *Method and system for operating a multilevel inverter*. US Patent, no. 20160126862, 2015.
6. Savitha M., Nagaraja Rao S. Switching angle optimization and fault analysis of a multistring-multilevel inverter for renewable-energy-source applications. *Clean Energy*, 2022, vol. 6, no. 6, pp. 907-930. doi: https://doi.org/10.1093/ce/zkac055.
7. Srinivas G., Durga Sukumar G., Subbarao M. Total harmonic distortion analysis of inverter fed induction motor drive using neuro fuzzy type-1 and neuro fuzzy type-2 controllers. *Electrical Engineering & Electromechanics*, 2024, no. 1, pp. 10-16. doi: https://doi.org/10.20998/2074-272X.2024.1.02.
8. Shanono I.H., Abdullah N.R.H., Daniyal H., Muhammad A. Selective harmonic elimination (SHE) based 3-phase multilevel voltage source inverter (VSI) for standalone applications. *SN Applied Sciences*, 2019, vol. 1, no. 12, art. no. 1670. doi: https://doi.org/10.1007/s42452-019-1726-3.
9. Muralikumar K., Ponnambalam P. Analysis of Cascaded Multilevel Inverter with a Reduced Number of Switches for Reduction of Total

Harmonic Distortion. *IETE Journal of Research*, 2023, vol. 69, no. 1, pp. 295-308. doi: https://doi.org/10.1080/03772063.2020.1819450.
10. Siddique M.D., Mekhilef S., Rawa M., Wahyudie A., Chokaev B., Salamov I. Extended Multilevel Inverter Topology With Reduced Switch Count and Voltage Stress. *IEEE Access*, 2020, vol. 8, pp. 201835-201846. doi: https://doi.org/10.1109/ACCESS.2020.3026616.
11. Nishizawa K., Itoh J., Odaka A., Toba A., Umida H. Input Current Harmonic Reduction based on Space Vector PWM for Three-level Inverter Operating over a Wide Range Power Factor. *IEEJ Journal of Industry Applications*, 2020, vol. 9, no. 3, pp. 208-218. doi: https://doi.org/10.1541/ieejjia.9.208.
12. Iqbal W., Qureshi I.M., Majeed H.B.A., Khan A. Performance Evaluation of Third Harmonic Injection PWM Technique for Three Phase Multilevel Inverter. *2021 International Conference on Frontiers of Information Technology (FIT)*, 2021, pp. 78-83. doi: https://doi.org/10.1109/FIT53504.2021.00024.
13. Xu J., Soeiro T.B., Gao F., Tang H., Bauer P. Carrier-Based Generalized Discontinuous PWM Strategy for Single-Phase Three-Legs Active Power Decoupling Converters. *IEEE Transactions on Industrial Electronics*, 2021, vol. 68, no. 11, pp. 11609-11613. doi: https://doi.org/10.1109/TIE.2020.3038099.
14. Gireesh Kumar D., Venkata Sireesha N., Ganesh A., Kotb H., AboRas K.M., Zeinoddini-Meymand H., Kamel S. Design of an Optimized Asymmetric Multilevel Inverter with Reduced Components Using Newton-Raphson Method and Particle Swarm Optimization. *Mathematical Problems in Engineering*, 2023, pp. 1-18. doi: https://doi.org/10.1155/2023/9966708.
15. Ebrahimi F., Windarko N.A., Gunawan A.I. Minimizing Total Harmonic Distortion of 7-Level Packed U-Cell Multilevel Inverter Using Whale Optimization Algorithm. *Indonesian Journal of Computer Science*, 2023, vol. 12, no. 6, pp. 3217-3231. doi: https://doi.org/10.33022/ijcs.v12i6.3507.
16. Ebrahimi F., Windarko N.A., Gunawan A.I. Reducing THD of 7-Level Packed U-cell Multilevel Inverter Using Genetic Algorithm. *2023 International Electronics Symposium (IES)*, 2023, pp. 88-93. doi: https://doi.org/10.1109/IES59143.2023.10242460.
17. Ahamad I., Ansari A.J., Iqbal A. THD Analysis of 5-Level, 7-Level and 9-Level CHB-Multilevel Inverters Using SPWM Switching Approach. *Lecture Notes in Electrical Engineering*, vol. 723 LNEE, pp. 719-728. doi: https://doi.org/10.1007/978-981-33-4080-0_69.
18. Izzaqi F.A., Windarko N.A., Qudsi O.A. Minimization of total harmonic distortion in neutral point clamped multilevel inverter using grey wolf optimizer. *International Journal of Power Electronics and Drive Systems (IJPEDS)*, 2022, vol. 13, no. 3, pp. 1486-1497. doi: https://doi.org/10.11591/ijpeds.v13.i3.pp1486-1497.
19. Ait bellah F., Abouloifa A., Echalih S., Hekss Z., Naftahi K., Lachkar I. Control Design of a Seven-Level Packed U Cell Inverter. *IFAC-PapersOnLine*, 2022, vol. 55, no. 12, pp. 677-682. doi: https://doi.org/10.1016/j.ifacol.2022.07.390.
20. Naruei I., Keynia F. Wild horse optimizer: a new meta-heuristic algorithm for solving engineering optimization problems. *Engineering with Computers*, 2022, vol. 38, no. S4, pp. 3025-3056. doi: https://doi.org/10.1007/s00366-021-01438-z.

F. Ebrahimi[1], M. Eng.,
N.A. Wndarko[1], PhD, Professor,
A.I. Gunawan[1], PhD, Doctor,
[1] Politeknik Elektronika Negeri Surabaya,
Raya ITS Str., Surabaya, 60111, Indonesia,
e-mail: faizuddin@pasca.student.pens.ac.id (Corresponding Author);
Ayub@pens.ac.id; Agus_ig@pens.ac.id